Terahertz Rectennas on Flexible Substrates Based on One-Dimensional Metal–Insulator–Graphene Diodes

Downloaded from: https://research.chalmers.se, 2026-09-09 13:02 UTC

Citation for the original published paper (version of record):
Hemmeter, A., Yang, X., Wang, Z. et al (2021). Terahertz Rectennas on Flexible Substrates Based on One-Dimensional Metal–Insulator–Graphene
Diodes. ACS Applied Electronic Materials, 3(9): 3747-3753.
http://dx.doi.org/10.1021/acsaelm.1c00134

N.B. When citing this work, cite the original published paper.

research.chalmers.se offers the possibility of retrieving research publications produced at Chalmers University of Technology. It covers all kind of research output: articles, dissertations, conference papers, reports etc. since 2004. research.chalmers.se is administrated and maintained by Chalmers Library

(article starts on next page)

ACS APPLIED ELECTRONIC MATERIALS

pubs.acs.org/acsaelm Letter

Terahertz Rectennas on Flexible Substrates Based on One-Dimensional Metal–Insulator–Graphene Diodes

Andreas Hemmetter, Xinxin Yang, Zhenxing Wang,* Martin Otto, Burkay Uzlu, Marcel Andree, Ullrich Pfeiffer, Andrei Vorobiev, Jan Stake, Max C. Lemme, and Daniel Neumaier

Cite This: ACS Appl. Electron. Mater. 2021, 3, 3747–3753

Read Online

ACCESS | Metrics & More | Article Recommendations | Supporting Information

ABSTRACT: Flexible energy harvesting devices fabricated in scalable thin-film processes are crucial for wearable electronics and the Internet of Things. We present a flexible rectenna based on a one-dimensional junction metal–insulator–graphene diode, offering low-noise power detection at terahertz (THz) frequencies. The rectennas are fabricated on a flexible polyimide film in a scalable process by photolithography using graphene grown by chemical vapor deposition. A one-dimensional junction reduces the junction capacitance and enables operation up to 170 GHz. The rectenna shows a maximum responsivity of 80 V/W at 167 GHz in free space measurements and minimum noise equivalent power of 80 pW/$\sqrt{\text{Hz}}$.

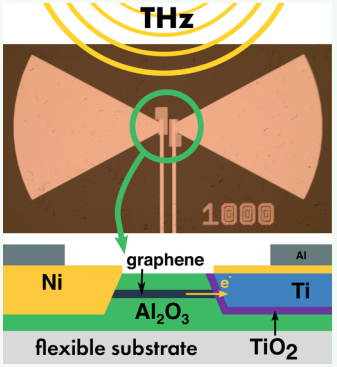

KEYWORDS: *graphene, terahertz detector, rectenna, metal–insulator–graphene diode*

See https://pubs.acs.org/sharingguidelines for options on how to legitimately share published articles.

Terahertz (THz) radiation is a region of the electromagnetic spectrum with frequencies between 0.1 and 10 THz.[1−3] Miniaturized THz sources and detectors enable a variety of applications, such as communications, surveillance screening, material analysis, biomedical diagnostics, and personal healthcare tracking.[1,2,4,5] The emergence of wearable electronics and networks of small, independent sensors for Internet of Things (IoT) applications is driving research both in low power electronic circuits and in energy harvesting on the device or chip level. Miniaturized THz power detectors may become crucial components that can function as energy harvesting devices, in particular on flexible thin-film substrates, where they can overcome the form factor limitations of silicon (Si) electronic chips and can be fabricated in scalable roll-to-roll processes. Thus, they have the potential to power decentralized sensor networks, passive readout circuits or integrated mobile devices without the need for batteries or an external power supply.[6]

Rectennas—antenna-coupled diodes—are versatile two-terminal devices that directly rectify a detected signal. Their zero-bias operation makes them suitable for energy harvesting applications.[7,8] This principle has been well established in the microwave region since 1966[9] because of the availability of Schottky diodes with sufficiently short response times.[10]

Increased cutoff frequencies in the THz range[11] have been achieved by metal–insulator–metal (MIM) diodes, which utilize tunneling and thermionic majority carrier conduction. However, MIM diodes generally show inferior DC performance compared to conventional p–n junction or Schottky diodes.[12] Metal–insulator–graphene (MIG) diodes (Figure 1a), where the cathode metal of a MIM diode is replaced by graphene, combine excellent DC performance with high cutoff frequencies.[12−15] The high charge carrier mobility and flexibility of graphene[15] allow such devices to be used in flexible THz rectennas, an application space that has been inaccessible due to the rigidity, bias and fabrication requirements of conventional semiconductor-based detectors. We present rectennas based on edge-contacted MIG diodes (Figure 1b), fabricated in a scalable thin-film compatible process, enabling high-throughput fabrication. The results point toward the possibility to integrate rectenna arrays as power supplies in flexible, wearable and conformal devices, for example wearable biomedical or distributed environmental sensors.

The operation frequency of a diode can be estimated using

$$f_c = \frac{1}{2\pi R_s C_b} \tag{1}$$

where R_s is the access resistance and C_b is the barrier capacitance from the diode's equivalent circuit seen in Figure

Received: February 9, 2021
Accepted: August 24, 2021
Published: August 27, 2021

© 2021 The Authors. Published by American Chemical Society

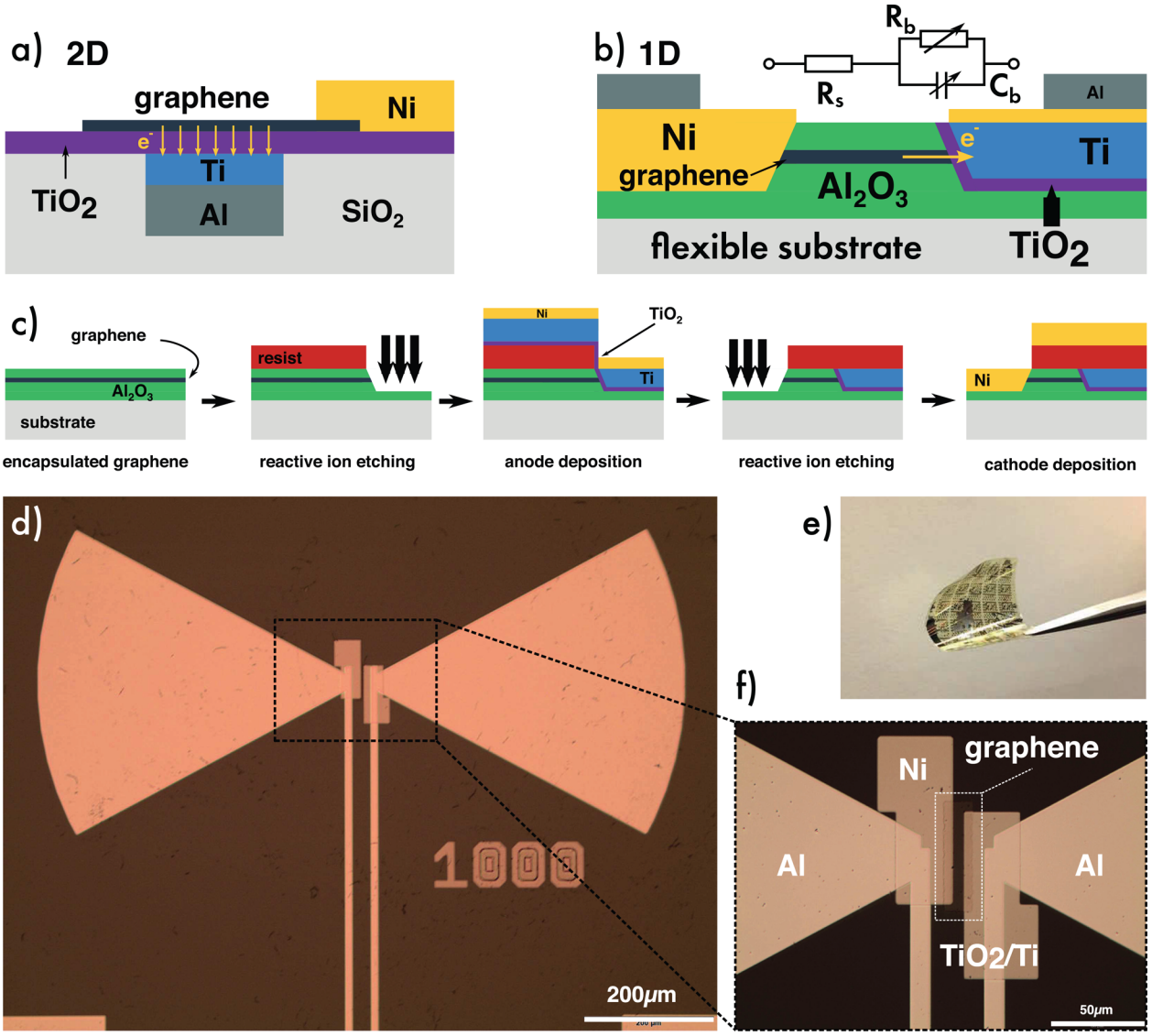

Figure 1. Rectenna structure and fabrication. (a) Cross-section of a 2D-MIG diode compared to a (b) 1D-MIG diode with equivalent circuit. (c) Key fabrication steps for the 1D-MIG diode. (d) Micrograph of a rectenna on polyimide. (e) Photograph of the sample on polyimide after peeling it off the Si carrier substrate. (f) Close-up of a 1D-MIG diode at the antenna feedpoint.

1b.[15,16] The low access resistance of conventional MIM diodes allows them to reach very high cutoff frequencies in the THz range, however with rather poor rectification performance.[12] MIG diodes, which have a similar layout as MIM diodes (Figure 1a), offer better rectification, but at the expense of a larger access resistance and therefore lower operation speed, as one metal layer is replaced by graphene. Furthermore, the current through a two-dimensional (2D) MIG diode is emitted perpendicularly to the graphene plane across a small "van-der-Waals gap" and is, therefore, affected by surface species at the graphene−insulator interface. This can increase the junction resistance, hindering an efficient coupling between antenna and diode.[14]

By forming a one-dimensional (1D) diode junction only to the graphene edge, as shown in the schematic cross-section in Figure 1b, the junction capacitance can be significantly reduced, enabling operation frequencies up to the THz range.[17] The effective junction area is then given by $A = w \times t$, where w is the channel width and t is the thickness of graphene, about 0.3 nm. This leads simultaneously to a reduced junction capacitance (C_b),[15] improved current injection at the insulator−graphene and graphene−metal interfaces and reduced operating voltage because of the electric field enhancement at the 1D edge.[17] On the other hand, the access resistance, as well as the junction resistance, is also reduced largely because of the edge contact. Edge contacts between graphene and a metal reduce the contact resistance by one order of magnitude compared to top contacts, which in the end contributes to reduce the access resistance.[18] By comparing the current density of the 1D- and 2D-MIG diodes, we can get an idea about the total resistance (the sum of access resistance and junction resistance), which is in fact dominated by the junction resistance. The thickness of graphene (0.3 nm) can be used to estimate the current density at the junction for 1D-MIG diode. A typical current density for a 1D-MIG diode is on the order of 10^6 A/cm^2, whereas that of a 2D-MIG diode reaches 3.8 A/cm^2 on average.[15] A field-effect device with edge contacts at both sides has been fabricated as a control device, whose schematic and characteristics are shown in the Supporting Information (Figures S1 and S2). An experimental

https://doi.org/10.1021/acsaelm.1c00134
ACS Appl. Electron. Mater. 2021, 3, 3747−3753

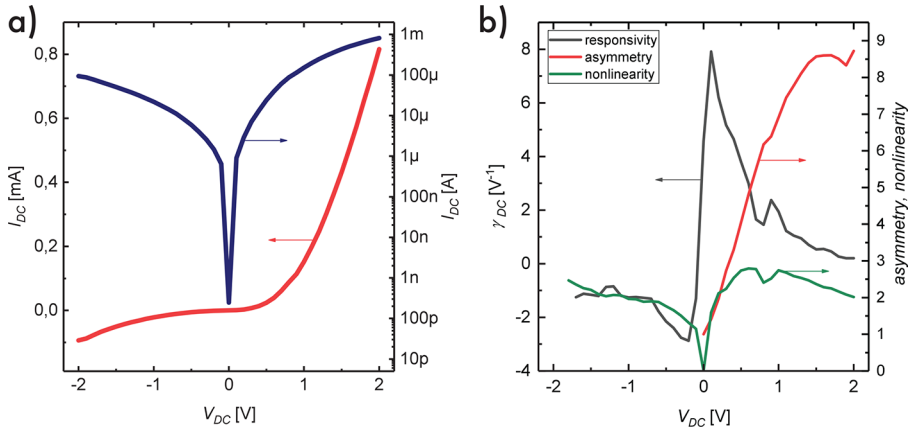

Figure 2. DC characteristics of a diode on a polyimide film. (a) Linear (blue) and logarithmic (red) $I-V$ curve and (b) derived figures of merit: responsivity γ_{DC} (black), asymmetry (red), and nonlinearity (green).

extraction of the circuit parameters of 1D-MIG diode up to 70 GHz has been shown previously.[15]

The rectennas consist of edge-contacted metal−insulator−graphene diodes at the feedpoint of broadband bowtie antennas. The rectennas have been fabricated on THz-transparent polyimide (PI) films on silicon handling substrates using standard microprocessing techniques such as contact photolithography and reactive ion etching. Key fabrication steps are shown in Figure 1c. The PI has first been covered with an aluminum oxide (Al_2O_3) layer through plasma-enhanced atomic layer deposition (ALD). CVD-grown graphene has been transferred in a wet process[19] onto the substrate and encapsulated with 20 nm Al_2O_3 in a thermal ALD process. A photolithographically defined mask has been used for reactive ion etching (RIE) through the Al_2O_3 and the graphene. The resist remains on the chip at this point and acts as a lift-off mask for the subsequent atomic layer deposition of 5 nm TiO_2 insulator, 20 nm sputtered titanium (Ti) anode metal[14,15] and 13 nm nickel (Ni). The self-aligned nature of the process prevents contamination of the graphene edge from photoresist residues or misalignment of graphene and metal layers, which would increase the diodes' capacitance and resistance. This process results in a one-dimensional MIG junction, because only the graphene edge is in electrical contact with the TiO_2 barrier (Figure 1b), as opposed to the two-dimensional contact in conventional MIG stacks (Figure 1a). A 25 nm thick Ni contact to the graphene has been fabricated in a similar way, that is, by reactive ion etching through the Al_2O_3/graphene/Al_2O_3 stack and subsequent metal deposition. Here, the graphene edge is in direct contact with the Ni and forms an ohmic contact.[15,20] At this point, graphene still covers the entire chip apart from directly below both metal contacts. The remaining graphene has been patterned into 6 μm long and 50 μm wide channels, before 100 nm thick aluminum (Al) has been deposited as antennas, transmission lines, and contact pads.

A key feature of the presented metal−insulator−graphene rectenna is that it is compatible with conventional thin-film technologies, that is, it does not involve high temperature processing steps >300 °C and uses only micrometer-scale lithography. A micrograph of a fabricated rectenna is shown in Figure 1d. The polyimide film is removed from the Si carrier substrate after the device fabrication for electrical measurements. Figure 1e shows a flexible PI substrate with several THz rectennas. A close-up of the finished diode on a flexible substrate is shown in Figure 1f.

The transmission behavior of the antennas was designed for broadband absorption to match the measurement setup tailored to the D band from 110 to 170 GHz. The parameter space was modeled using the electromagnetic finite element solver HFSS with a lumped port (Z_a = 377 Ω) at the feedpoint. The chosen bowtie antenna design with an opening angle of 30° has a large bandwidth of 43% at 157 GHz (defined as a voltage standing wave ratio VSWR ≤ 2), enabling free space measurements over the D band from 110 to 170 GHz. A pair of 1 mm long metal traces lead from the diode contacts to larger contact pads for biasing and signal readout. The transmission line serves as a low-pass filter that rejects the received THz signal and only allows the rectified DC component to pass.

Direct current (DC) characteristics of the rectennas have been measured under ambient conditions. Current−voltage ($I-V$) measurements, where the bias voltage V_{DC} has been swept from −2 to +2 V, are shown linearly and logarithmically in Figure 2a. The device shows a nonlinear $I-V$ characteristic and reaches maximum currents of I_{DC} = 0.8 mA at a forward bias voltage of V_{DC} = 2 V and I_{DC} = 0.1 mA at V_{DC} = −2 V. Typically, such currents are normalized by the device dimensions in order to compare them to the state of the art. Here, only the graphene edge emits charge carriers across the barrier. Taking into account the graphene thickness of approximately 0.3 nm and the device width of 50 μm, the resulting maximum current density at the graphene edge exceeds 5 × 10^6 A/cm^2 in the forward direction, consistent with previously reported 1D-MIG diodes by Wang et al.[15]

The $I-V$ curve allows calculating the responsivity γ_{DC} of the diode, one of the decisive figures of merit for RF applications. The responsivity is a measure for the rectification efficiency of the diode:[14]

$$\gamma_{dc} = \frac{d^2I/dV^2}{dI/dV} \tag{2}$$

As can be seen from its expanded units $\left(\frac{1}{V} = \frac{A}{VA} = \frac{A}{W}\right)$, a diode's responsivity is related to the rectified current at a given input power. The flexible diode reaches a maximum responsivity of 8 V^{-1} (Figure 2b) in the vicinity of V_{DC} = 0 V. Beyond the $I-V$ curve and the responsivity, further important figures of merit are the asymmetry and the

https://doi.org/10.1021/acsaelm.1c00134
ACS Appl. Electron. Mater. 2021, 3, 3747−3753

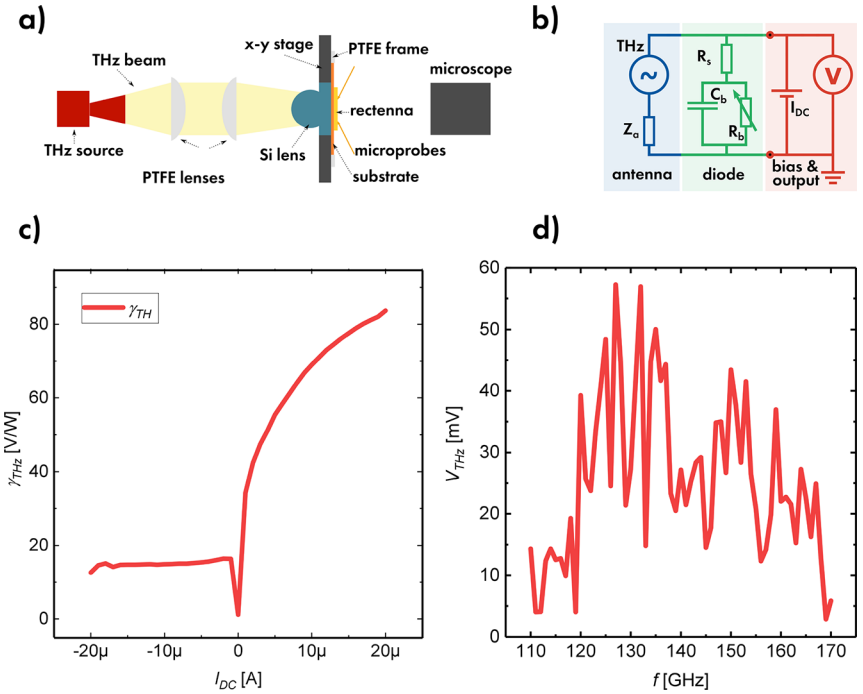

Figure 3. THz measurement of a flexible rectenna. (a) Schematic of the free-space measurement setup and (b) equivalent circuit of the system. (c) Bias current dependency of the voltage responsivity. (d) Frequency dependency of the rectified voltage under illumination with THz radiation.

nonlinearity of the diode. The asymmetry is the ratio between forward and reverse current $\left(f_{\text{asym}} = \left|\frac{I_F}{I_R}\right|\right)$, while the nonlinearity is given by $f_{\text{NL}} = \frac{dI}{dV}/\frac{I}{V}$. Both quantities are shown additionally in Figure 2b.

Measurements at THz frequencies between 110 and 170 GHz were conducted in free space under ambient conditions. A sine-wave modulated THz signal (333 Hz) was transmitted by a horn antenna, collimated, and prefocused by two identical PTFE (Teflon) lenses and finally focused onto the back of the sample by a hyper-hemispherical Si lens. The setup is shown schematically in Figure 3a. After peeling off the PI film from the Si substrate, the flexible chip was mounted onto a high-resistivity Si lens in the beam path. Microprobes contacted the sample behind the beam path. A Keithley 2604B source meter provided the DC input bias as a current through an external resistor and simultaneously measured the DC voltage at the diode. The THz source was composed of a VDI WR6.5SGX extender driven by an Agilent 83650A signal generator with 30 dB sine wave modulation at 333 Hz. The rectified voltage response was measured using an SR830 lock-in amplifier. For calibration, the available output power of the extender P_{ava} across the D band was measured using an Erickson calorimetric power meter directly at the waveguide flange of the extender on which the horn antenna was mounted. To describe the diode's behavior during THz measurement we formulate a small-signal equivalent circuit, shown in Figure 3b.

A key THz detector characteristic is the optical voltage responsivity γ_{THz}, which is defined in eq 3 as the DC output voltage per THz power and is given in units of [V/W]:

$$\gamma_{\text{THz}} = \frac{2\sqrt{2}\,\Delta V}{P_{\text{ava}}} = \beta_{\text{THz}} R \tag{3}$$

Here, ΔV is the rectified DC voltage measured by the lock-in amplifier.[21] The optical current responsivity β_{THz} in [A/W] can be calculated from the voltage responsivity and the total diode resistance R at the respective operating point. The prefactors originate in the peak-to-peak and root-mean-square (rms) amplitudes of the lock-in amplifier.[21] The bias-dependent THz response was measured at 167 GHz with a THz output power P_{ava} = 1 mW. The maximum optical voltage responsivity γ_{THz} = 83.7 V/W was reached at an applied bias current of 20 μA and a measured DC voltage of 1.47 V (Figure 3c). This corresponds to an optical current responsivity β_{THz} = 1.13 mA/W at a total device resistance R = 74 kΩ.

It is noticeable that the optical responsivity under THz measurements increases with applied bias, while the DC responsivity shows a peak close to zero bias. This can be explained by the nonideal impedance matching between diode and antenna. As a higher bias is applied, the junction resistance of the diode decreases, thus better matching its impedance to that of the antenna, and increasing the power delivered to the diode. The matching between antenna and diode can be improved through a dedicated matching network, for example, based on graphene-based passive components, as demonstrated in previous work.[22,23]

The rectified voltage over the D band from 110 to 170 GHz is shown in Figure 3d. During the frequency sweep the bias current was fixed at −10 μA and the rectified voltage was recorded. The voltage V_{THz} does not show any noticeable frequency dependency, but fluctuations, because of the uneven power output of the THz source, and the interferences in the polyimide film as well as between the components in the beam path. We expect that measuring the device at different distances from the source can mitigate these fluctuations, although the practical measurement would require precise and repeatable alignment of the sample to the beam path. The Teflon and silicon lenses used to focus the THz beam contribute an absorption loss of around 3 dB, and a further unknown part of the beam is reflected or scattered at various interfaces without contributing to the incident power. Even

https://doi.org/10.1021/acsaelm.1c00134
ACS Appl. Electron. Mater. 2021, 3, 3747−3753

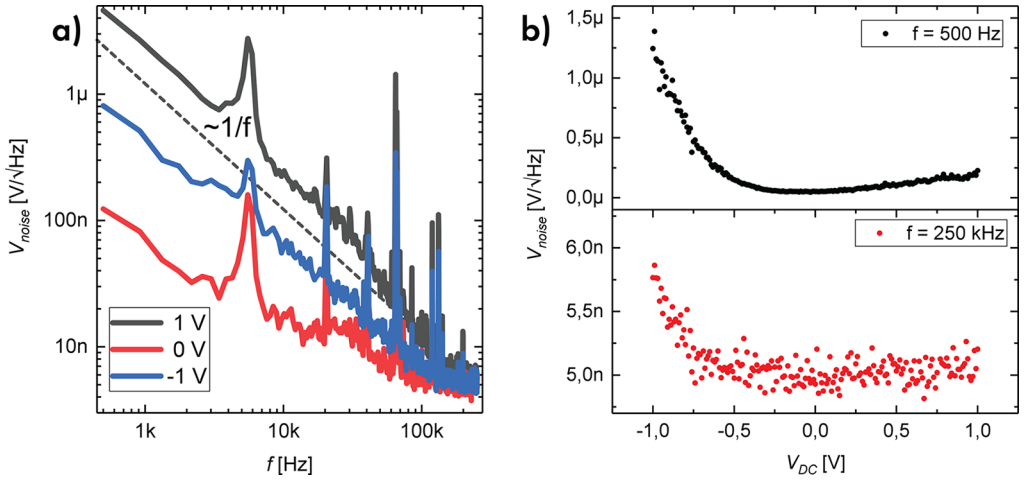

Figure 4. Noise measurements. (a) Voltage noise spectrum from 500 Hz to 250 kHz, measured on-chip. (b) Bias dependence of the voltage noise at 500 Hz (top) and 250 kHz (bottom).

Table 1. Comparison to Other THz Detectors from Literature[a]

	detector + antenna	f [GHz]	γ_{THz} [V/W]	NEP [pW/√Hz]	diode	flexible	ref
	MIM + bowtie[b]	28300	0.2		√		24
	traveling wave MIM + bowtie[b]	28300	0.3		√		25
⬡	GFET + bowtie	487	2	3000		√	21
	CNT Schottky	540	2.6	20000			26
⬡	photothermoelectric	2519	10	1100			27
	MSM + log spiral[b]	300	10.8	100	√		28
⬡	flexible 1D-MIG + bowtie	167	83.7	81 (3500)	√	√	
	unipolar nanodiode + bowtie	1500	300	330	√		29
⬡	photothermoelectric[b]	2519	715	16			27
⬡	ballistic diode + bowtie[b]	685	764	34	√		30

[a]The rectenna discussed in this work is highlighted in grey. The hexagon in the first column indicates if the detector is based on graphene. The detectors marked with an asterisk use the actual incident power on the device, rather than the emitted power of the source. The values reported for our detector come from the total emitted power P_{ava} from the source and are thus likely underestimated. The NEP of the device from this work was measured at 250 kHz. The NEP at a frequency of 500 Hz is provided in parentheses as a comparison. [b]Responsivity calculated from incident or absorbed rather than emitted power.

though the substrate materials are transparent to radiation in the THz regime, the mismatch in refractive indices introduces undesirable frequency dependent reflections that reduce the RF intensity at the rectenna. As such, the measured value is a lower bound of the optical responsivity.

A test device with ground-signal-ground pads and an identical diode to the one in the rectenna has been fabricated to measure the voltage noise V_{noise} directly on-chip. Figure 4a shows the noise at different bias levels at frequencies between 500 Hz and 250 kHz. The bias dependence of the voltage noise is shown in Figure 4b. The noise equivalent power (NEP = V_{noise}/γ_{THz}) of the detector can be calculated from the voltage noise V_{noise} and the responsivity γ_{THz}. At 250 kHz (500 Hz), the minimum NEP is 81.0 pW/√Hz (3.5 nW/√Hz) at a bias voltage of 1 V and 4.3 nW/√Hz (44.1 nW/√Hz) at zero bias.

The rectenna performance under bending can be deduced from the behavior of the individual components, that is, the diode and the antenna. A similar 1D-MIG diode has been demonstrated to retain its characteristics even after 1000 bending cycles with a bending radius of 6.4 mm.[15] The performance of the antenna under bending has been modeled in HFSS by folding each arm of the antenna by an angle of 2.8° with respect to the horizontal, approximating (first-order) the bending of the device by 0.06%, just as the 1D-MIG diode mentioned above.[15] The VSWR does not differ significantly from that in the flat state (Figure S3). With the experimental verification of the diode and the simulation of the antenna, we can conclude that such a rectenna can in principle still function at least to a bending radius of 6.4 mm, corresponding to a strain of 0.06%.

Table 1 compares our rectenna on a flexible substrate to other THz detectors from literature. The rectenna shows a higher responsivity than MIM or metal−semiconductor−metal (MSM) based rectennas, despite being fabricated on a flexible substrate. It also outperforms the only other reported flexible THz detector by Yang et al. based on a graphene field-effect transistor[21] and most other THz detectors based on the absorption effects. It should be noted that many references derive values for the optical responsivity from the incident or absorbed power on the device area. Since our reported optical responsivity uses the *total emitted* power P_{ava} from the source (not scaled to the device area), it represents a lower bound that is mainly limited by the impedance mismatch between diode and antenna and absorption and scattering in the beam path.

In summary, we have demonstrated detection of THz signals through an edge-contacted graphene-based rectenna in free space measurements. The flexible rectenna, fabricated using scalable, thin-film compatible processes and CVD-grown

https://doi.org/10.1021/acsaelm.1c00134
ACS Appl. Electron. Mater. 2021, 3, 3747−3753

graphene, reaches a responsivity of 83.7 V/W at 167 GHz with a NEP of 81.0 pW/$\sqrt{\text{Hz}}$, enabling low-cost energy harvesting at the chip level in flexible electronics.

■ ASSOCIATED CONTENT

Supporting Information

The Supporting Information is available free of charge at https://pubs.acs.org/doi/10.1021/acsaelm.1c00134.

Graphene channel transfer measurements, including schematic of the measurement setup and measured transfer curve, and modeled antenna performance under bending (PDF)

■ AUTHOR INFORMATION

Corresponding Author

Zhenxing Wang − *Advanced Microelectronic Center Aachen (AMICA), AMO GmbH, 52074 Aachen, Germany;* orcid.org/0000-0002-2103-7692; Email: wang@amo.de

Authors

Andreas Hemmetter − *Advanced Microelectronic Center Aachen (AMICA), AMO GmbH, 52074 Aachen, Germany; Chair of Electronic Devices, Faculty of Electrical Engineering and Information Technology, RWTH Aachen University, 52074 Aachen, Germany*

Xinxin Yang − *Department of Microtechnology and Nanoscience, Chalmers University of Technology, SE-41296 Gothenburg, Sweden;* orcid.org/0000-0003-4464-6922

Martin Otto − *Advanced Microelectronic Center Aachen (AMICA), AMO GmbH, 52074 Aachen, Germany*

Burkay Uzlu − *Advanced Microelectronic Center Aachen (AMICA), AMO GmbH, 52074 Aachen, Germany; Chair of Electronic Devices, Faculty of Electrical Engineering and Information Technology, RWTH Aachen University, 52074 Aachen, Germany;* orcid.org/0000-0001-6776-8901

Marcel Andree − *Institute for High-Frequency and Communication Technology, University of Wuppertal, 42119 Wuppertal, Germany*

Ullrich Pfeiffer − *Institute for High-Frequency and Communication Technology, University of Wuppertal, 42119 Wuppertal, Germany*

Andrei Vorobiev − *Department of Microtechnology and Nanoscience, Chalmers University of Technology, SE-41296 Gothenburg, Sweden;* orcid.org/0000-0003-2882-3191

Jan Stake − *Department of Microtechnology and Nanoscience, Chalmers University of Technology, SE-41296 Gothenburg, Sweden;* orcid.org/0000-0002-8204-7894

Max C. Lemme − *Advanced Microelectronic Center Aachen (AMICA), AMO GmbH, 52074 Aachen, Germany; Chair of Electronic Devices, Faculty of Electrical Engineering and Information Technology, RWTH Aachen University, 52074 Aachen, Germany*

Daniel Neumaier − *Chair of Smart Sensor Systems, University of Wuppertal, 42119 Wuppertal, Germany; Advanced Microelectronic Center Aachen (AMICA), AMO GmbH, 52074 Aachen, Germany*

Complete contact information is available at: https://pubs.acs.org/10.1021/acsaelm.1c00134

Author Contributions

The experiments have been conceived by A. H., Z. W., M. L., and D. N. A. H. designed the devices and performed the electrical characterization. A. H., M. O., and B. U. fabricated the devices. X. Y. performed the electrical and optical characterization. M. A. performed the noise measurement. All authors contributed to discussions and the analysis and interpretation of the results. All authors have given approval to the final version of the manuscript.

Notes

The authors declare no competing financial interest.

■ ACKNOWLEDGMENTS

This project has received funding from the European Union's Horizon 2020 research and innovation programme under grant agreement No. 101006963 (GreEnergy), No. 881603 (Graphene Flagship), and No. 863337 (WiPLASH). This research was further financially supported by the DFG projects HiPeDi (No. WA4139/1.1), GLECS-2 (No. NE1633/3).

■ REFERENCES

(1) Tonouchi, M. Cutting-edge terahertz technology. *Nat. Photonics* **2007**, *1*, 97−105.

(2) Siegel, P. H. Terahertz technology. *IEEE Trans. Microwave Theory Tech.* **2002**, *50*, 910−928.

(3) Mittleman, D., Ed. *Sensing with Terahertz Radiation*; Springer: Berlin, 2003.

(4) Sizov, F.; Rogalski, A. THz detectors. *Prog. Quantum Electron.* **2010**, *34*, 278−347.

(5) Huang, X.; Leng, T.; Zhu, M.; Zhang, X.; Chen, J.; Chang, K.; Aqeeli, M.; Geim, A. K.; Novoselov, K. S.; Hu, Z. Highly Flexible and Conductive Printed Graphene for Wireless Wearable Communications Applications. *Sci. Rep.* **2016**, *5*, 18298.

(6) Haring Bolívar, P.; Nagel, M.; Richter, F.; Brucherseifer, M.; Kurz, H.; Bosserhoff, A.; Büttner, R. Label-Free THz Sensing of Genetic Sequences: Towards 'THz Biochips'. *Philos. Trans. R. Soc., A* **2004**, *362*, 323−335.

(7) Moddel, G., Grover, S., Eds. *Rectenna Solar Cells*; Springer: New York, 2013.

(8) Zhu, Z.; Joshi, S.; Grover, S.; Moddel, G. Graphene geometric diodes for terahertz rectennas. *J. Phys. D: Appl. Phys.* **2013**, *46*, 185101.

(9) Brown, W.; Mims, J.; Heenan, N. An experimental microwave-powered helicopter. *1958 IRE International Convention Record*, 1965; pp 225−235.

(10) Pfeiffer, U. R.; Mishra, C.; Rassel, R. M.; Pinkett, S.; Reynolds, S. K. Schottky Barrier Diode Circuits in Silicon for Future Millimeter-Wave and Terahertz Applications. *IEEE Trans. Microwave Theory Tech.* **2008**, *56*, 364−371.

(11) Gadalla, M. N.; Abdel-Rahman, M.; Shamim, A. Design, Optimization and Fabrication of a 28.3 THz Nano-Rectenna for Infrared Detection and Rectification. *Sci. Rep.* **2015**, *4*, 4270.

(12) Shriwastava, S.; Tripathi, C. C. Metal−Insulator−Metal Diodes: A Potential High Frequency Rectifier for Rectenna Application. *J. Electron. Mater.* **2019**, *48*, 2635−2652.

(13) Urcuyo, R.; Duong, D. L.; Jeong, H. Y.; Burghard, M.; Kern, K. High Performance Graphene-Oxide-Metal Diode through Bias-Induced Barrier Height Modulation. *Advanced Electronic Materials* **2016**, *2*, 1600223.

(14) Shaygan, M.; Wang, Z.; Elsayed, M. S.; Otto, M.; Iannaccone, G.; Ghareeb, A. H.; Fiori, G.; Negra, R.; Neumaier, D. High performance metal−insulator−graphene diodes for radio frequency power detection application. *Nanoscale* **2017**, *9*, 11944−11950.

(15) Wang, Z.; Uzlu, B.; Shaygan, M.; Otto, M.; Ribeiro, M.; Marín, E. G.; Iannaccone, G.; Fiori, G.; Elsayed, M. S.; Negra, R.; Neumaier, D. Flexible One-Dimensional Metal−Insulator−Graphene Diode. *ACS Applied Electronic Materials* **2019**, *1*, 945−950.

(16) Cowley, A. M.; Sorensen, H. O. Quantitative Comparison of Solid-State Microwave Detectors. *IEEE Trans. Microwave Theory Tech.* **1966**, *14*, 588−602.

(17) Wang, L.; Meric, I.; Huang, P. Y.; Gao, Q.; Gao, Y.; Tran, H.; Taniguchi, T.; Watanabe, K.; Campos, L. M.; Muller, D. A.; Guo, J.; Kim, P.; Hone, J.; Shepard, K. L.; Dean, C. R. One-Dimensional Electrical Contact to a Two-Dimensional Material. *Science* **2013**, *342*, 614−617.
(18) Shaygan, M.; Otto, M.; Sagade, A. A.; Chavarin, C. A.; Bacher, G.; Mertin, W.; Neumaier, D. Low Resistive Edge Contacts to CVD-Grown Graphene Using a CMOS Compatible Metal. *Ann. Phys.* **2017**, *529*, 1600410.
(19) de la Rosa, C. J. L.; Lindvall, N.; Cole, M. T.; Nam, Y.; Löffler, M.; Olsson, E.; Yurgens, A. Frame assisted H2O electrolysis induced H2 bubbling transfer of large area graphene grown by chemical vapor deposition on Cu. *Appl. Phys. Lett.* **2013**, *102*, 022101.
(20) Kretz, B.; Pedersen, C. S.; Stradi, D.; Brandbyge, M.; Garcia-Lekue, A. Atomistic Insight into the Formation of Metal-Graphene One-Dimensional Contacts. *Phys. Rev. Appl.* **2018**, *10*, 024016.
(21) Yang, X.; Vorobiev, A.; Generalov, A.; Andersson, M. A.; Stake, J. A flexible graphene terahertz detector. *Appl. Phys. Lett.* **2017**, *111*, 021102.
(22) Saeed, M.; Hamed, A.; Wang, Z.; Shaygan, M.; Neumaier, D.; Negra, R. Graphene integrated circuits: new prospects towards receiver realisation. *Nanoscale* **2018**, *10*, 93−99.
(23) Wang, Z.; Hemmetter, A.; Uzlu, B.; Saeed, M.; Hamed, A.; Kataria, S.; Negra, R.; Neumaier, D.; Lemme, M. C. Graphene in 2D/3D Heterostructure Diodes for High Performance Electronics and Optoelectronics. *Advanced Electronic Materials* **2021**, *7*, 2001210.
(24) Jayaswal, G.; Belkadi, A.; Meredov, A.; Pelz, B.; Moddel, G.; Shamim, A. Optical rectification through an Al2O3 based MIM passive rectenna at 28.3 THz. *Materials Today Energy* **2018**, *7*, 1−9.
(25) Pelz, B.; Belkadi, A.; Moddel, G. Traveling-wave metal-insulator-metal diodes for infrared rectennas. *IEEE 43rd Photovoltaic Specialists Conference (PVSC)*, 2016.
(26) Manohara, H. M.; Wong, E. W.; Schlecht, E.; Hunt, B. D.; Siegel, P. H. Carbon Nanotube Schottky Diodes Using Ti-Schottky and Pt-Ohmic Contacts for High Frequency Applications. *Nano Lett.* **2005**, *5*, 1469−1474.
(27) Cai, X.; Sushkov, A. B.; Suess, R. J.; Jadidi, M. M.; Jenkins, G. S.; Nyakiti, L. O.; Myers-Ward, R. L.; Li, S.; Yan, J.; Gaskill, D. K.; Murphy, T. E.; Drew, H. D.; Fuhrer, M. S. Sensitive room-temperature terahertz detection via the photothermoelectric effect in graphene. *Nat. Nanotechnol.* **2014**, *9*, 814−819.
(28) Moon, K.; Shin, J.-H.; Lee, I.-M.; Park, D. W.; Lee, E. S.; Park, K. H. Terahertz rectifier exploiting electric field-induced hot-carrier effect in asymmetric nano-electrode. *Nanotechnology* **2018**, *29*, 47LT01.
(29) Balocco, C.; Kasjoo, S. R.; Lu, X. F.; Zhang, L. Q.; Alimi, Y.; Winnerl, S.; Song, A. M. Room-temperature operation of a unipolar nanodiode at terahertz frequencies. *Appl. Phys. Lett.* **2011**, *98*, 223501.
(30) Auton, G.; But, D. B.; Zhang, J.; Hill, E.; Coquillat, D.; Consejo, C.; Nouvel, P.; Knap, W.; Varani, L.; Teppe, F.; Torres, J.; Song, A. Terahertz Detection and Imaging Using Graphene Ballistic Rectifiers. *Nano Lett.* **2017**, *17*, 7015−7020.

https://doi.org/10.1021/acsaelm.1c00134
ACS Appl. Electron. Mater. 2021, 3, 3747−3753